Environmental Research 267 (2025) 120663

Contents lists available at ScienceDirect

Environmental Research

journal homepage: www.elsevier.com/locate/envres

Transcriptomic and physiological analyses reveal the toxic effects of inorganic filters (nZnO and $nTiO_2$) on scleractinian coral *Galaxea fascicularis*

Jian Chen [a], Kefu Yu [a,b,*], Xiaopeng Yu [a], Ruijie Zhang [a], Biao Chen [a]

[a] Guangxi Laboratory on the Study of Coral Reefs in the South China Sea, Coral Reef Research Center of China, School of Marine Sciences, Guangxi University, Nanning, 530004, China
[b] Southern Marine Science and Engineering Guangdong Laboratory (Guangzhou), Guangzhou, 511458, China

ARTICLE INFO

Keywords:
Inorganic UV filter
Sunscreens
Coral
Stress
Transcriptional responses

ABSTRACT

The effects of sunscreen on scleractinian corals have garnered widespread attention; however, the toxic effects and mechanisms remain unclear. This study investigated the toxicological effects of two common inorganic filters used in sunscreens, nano zinc oxide and titanium dioxide (nZnO and $nTiO_2$), on the reef-building coral *Galaxea fascicularis*, focusing on the phenotypic, physiological, and transcriptomic responses. The results showed that after exposure to 0.8 mg/L of nZnO and 30 mg/L of $nTiO_2$ for 48 h, all coral polyps exhibited retraction. Zn and Ti ions were detected in coral tissues at concentrations of 67.18 and 24.87 μg/g, respectively, indicating the accumulation of nZnO and $nTiO_2$ in coral tissues. The zooxanthellae density, *Fv/Fm*, and chlorophyll-*a* content decreased significantly. The activity of antioxidant enzymes showed an increasing trend. Meanwhile, glutamine synthetase and glutamate dehydrogenase activities exhibited a decreasing trend. The health status of corals was impacted as a result of nZnO and $nTiO_2$ stress. Transcriptomic analysis showed that the toxicity mechanisms of nZnO and $nTiO_2$ differed in corals. Following exposure to nZnO, differentially expressed genes (DEGs) in corals were mainly enriched in signaling pathways related to immune response. The genes related to innate immunity, such as *MASP1, MUC5AC, TLRs,* and *C2,* were significantly upregulated, indicating that nZnO exposure induces an innate immune response in corals. Meanwhile, following $nTiO_2$ exposure, the upregulated DEGs were mainly enriched in signaling pathways related to transporter activity. In contrast, the downregulated DEGs were mainly enriched in energy metabolism pathways, indicating that $nTiO_2$ disrupted the energy supply of corals, thereby leading to an increased demand for nutrient transport. This study reveals the toxic effects of nZnO and $nTiO_2$, and their mechanisms of action on scleractinian corals, providing a reference for further assessing the toxicity of sunscreen on corals.

1. Introduction

Over the past few decades, the global production and use of sunscreen have been increasing annually (Roberto et al., 2008). However, the negative effects of sunscreen on coral reef ecosystems have attracted widespread attention (Roberto et al., 2008). Approximately 6000 tons of sunscreen are released into the coral reef environment annually, and approximately 10% of coral reefs are threatened by sunscreen-induced coral bleaching (He et al., 2023; Roberto et al., 2008). Coral reef areas, such as Hanauma Bay in Hawaii, Maya Bay in Thailand, and Playa Delfines in Mexico, receive 2000–15,000 visitors daily during the peak tourist season, resulting in a sharp increase in the sunscreen components in the sea over relatively short timescales (Downs et al., 2011, 2021, 2022; Sendra et al., 2017). The concentration of sunscreen agents in the waters of the coral reef area in the US Virgin Islands reached 1.4 mg/L, leading to impaired coral larvae settlement, adult tissue regeneration and the death of juvenile corals (Downs et al., 2016; Vuckovic et al., 2022). By 2030, the number of global tourists visiting coastal regions is expected to exceed 3 billion, with 70 million visiting coral reefs. This increase in tourism activities poses a significant threat to the fragile coral reef ecosystems (Glaesser et al., 2017). Therefore, to protect coral reef ecosystems, some popular coral reef tourist attractions, such as Hawaii, Palau, and Mexico, have banned the use of sunscreens containing specific components, such as oxybenzone, ethylhexyl

* Corresponding author. Guangxi Laboratory on the Study of Coral Reefs in the South China Sea, Guangxi University, Nanning, China.
E-mail address: kefuyu@scsio.ac.cn (K. Yu).

https://doi.org/10.1016/j.envres.2024.120663
Received 10 October 2024; Received in revised form 2 December 2024; Accepted 17 December 2024
Available online 19 December 2024

methoxycinnamate, and octocrylene (BBC, 2018).

Ultraviolet filters (UVFs), the main components of sunscreen, are used for protection against ultraviolet radiation (Downs et al., 2022). They include active organic filters, such as benzophenones, camphor derivatives, and cinnamates, and inorganic filters, such as nanosize zinc oxide (nZnO) and titanium dioxide ($nTiO_2$). Some organic UVFs, such as oxybenzone and octinoxate are dangerous to marine ecosystems and have been forbidden in several countries (Moeller et al., 2021; Jiang et al., 2024). Due to their stable composition and broad-spectrum anti-UV effects, inorganic UVFs have replaced organic UVFs as the main components of sunscreen and other sun-protection products (Schneider and Lim, 2019; Yuan et al., 2022). Two metal oxide nanoparticles (NPs), nZnO and $nTiO_2$, are extensively used as inorganic UVFs and have been certified under applicable product safety regulations (Sanchez-Quiles and Tovar-Sanchez, 2014; Sendra et al., 2017). As micropollutants, UVFs can enter the marine environment directly through coastal activities, such as swimming, surfing, and diving, or indirectly through sewage treatment plant discharges, land runoff, and atmospheric deposition. The widespread presence of UVFs can harm marine ecosystems (Moeller et al., 2021; Roberto et al., 2008; Sanchez-Quiles and Tovar-Sanchez, 2014; Vuckovic et al., 2022). Due to direct application and indirect discharge, the concentration of $nTiO_2$ in aquatic environments can reach hundreds of thousands of μg/L in wastewater and several to dozens of μg/L in surface water (Li et al., 2022). It was found that TiO_2 and ZnO in the surface waters of French Mediterranean beaches were detected at concentrations of 900 and 15 μg/L, respectively (Labille et al., 2020), and the accumulated concentration of TiO_2 in surface sediments reached 40 mg/kg (Sun et al., 2016).

Previous studies have mainly focused on the toxic effects of organic UVFs on corals. However, there are few studies on the toxic effects of inorganic UVFs in sunscreen, such as nZnO and $nTiO_2$ on corals. nZnO and $nTiO_2$ have been labeled as "coral-safe" and "green" sunscreen ingredients; however, this is due to insufficient toxicity studies on corals (Yuan et al., 2023). Indeed, some studies have revealed that nZnO and $nTiO_2$ can cause significantly negative effects on marine ecosystems. It was found that 10 mg/L $nTiO_2$ or 1 mg/L nZnO significantly reduced the growth rate of phytoplankton communities (Takasu et al., 2023) and that ZnO in sunscreen can impact embryonic survival of the purple sea urchin (*Strongylocentrotus purpuratus*) by interfering with skeleton formation and axial determination (Cunningham et al., 2020). Furthermore, Wu et al., 2022 found that exposure to 100 μg/L nZnO caused oxidative injury to proteins and lipids and induced a marked apoptotic response in mussels (*Mytilus edulis*). Furthermore, there is concern that inorganic UVFs may accumulate in organisms and potentially undergo biomagnification through the marine food chain (Marcellini et al., 2024). With the increasing prevalence of coastal activities, a growing number of sunscreens containing nZnO and $nTiO_2$ are being introduced into coral reef waters. Therefore, it is necessary to further examine the toxic effects of nZnO and $nTiO_2$ on scleractinian corals. In addition, there is currently a lack of whole-genome assembly data on the toxic molecular mechanisms of nZnO and $nTiO_2$ in corals. Transcriptome analysis may provide new insights into the molecular mechanisms underlying inorganic UVFs toxicity in reef-building corals.

Galaxea fascicularis, a typical scleractinian coral, usually inhabits shallow waters (2–15 m deep) in tropical and subtropical regions. It is widely distributed in the Indo-Pacific region and plays a vital role in maintaining coral reef ecosystem functionality (Wang et al., 2022; Yu et al., 2021). *Galaxea fascicularis* has a relatively high tolerance and is readily grown and reproduced in aquariums. The polyp has a relatively large morphology, enabling easy separation and observation. Therefore, it is an excellent model species for research (Puntin et al., 2022). In the present study, we aimed to elucidate the toxic effects of inorganic UVF-induced acute stress on corals. We assessed the toxic effects of two typical sunscreen ingredients, nZnO and $nTiO_2$, on *G. fascicularis* through phenotypic, physiological, biochemical, and transcriptomic analyses and examined the key functional genes and signaling pathways.

2. Materials and methods

2.1. Particle characterization of nZnO and $nTiO_2$

$nTiO_2$ (purity >99.9%) and nZnO (purity >99.9%) powders were purchased from Shanghai Aladdin Biochemical Technology Co. Ltd. The following analyses were conducted on nZnO and $nTiO_2$: a morphological analysis using scanning electron microscopy (SEM) and a size distribution analysis using a laser diffraction particle size analyzer. The hydrodynamic size, degree of polymerization, and separation coefficient of the nZnO and $nTiO_2$ suspensions in Milli-Q water were measured using a multi-angle particle size and highly sensitive zeta potential analyzer (NanoBook Omni, Brookhaven, USA), and the zeta potentials of nZnO and $nTiO_2$ were determined using the same analyzer. The stock solution was sonicated using an ultrasonicator (kHz, 30 min, Qsonica Q700, Newtown, CT, U.S.A.) until the nanoparticles were well distributed and diluted to the desired concentration. This assay was performed as described previously (Wan et al., 2019).

2.2. Coral sample collection and experimental exposure

Galaxea fascicularis colonies were collected from Weizhou Island in the Beibu Gulf of China and temporarily maintained at the Coral Reef Research Center of Guangxi University, China. Sample collection was approved by the Management Office of the Beihai National Coral Reef Nature Reserve in China. Clones from the same isolate of *G. fascicularis* were selected to minimize potential individual and genetic variability. A larger colony of *G. fascicularis* was divided into fragments, each approximately 10 cm^2 in size, and then transferred into a 300-L aquarium illuminated with aquarium light consisting of a 250 W metal halogen lamp and four T5HO lamps that mimicked natural light with a 12 h light/12 h dark cycle. The corals were acclimated at 26 °C for 14 d before the experiment. During the experiment, the lighting and aquarium conditions remained unchanged. *Galaxea fascicularis* were fed freshly hatched *Artemia salina* nauplii (brine shrimp) twice weekly. The corals were given time to recover from fragmentation prior to the initiation of the pollution stress experiment.

Before the experiment, we conducted concentration gradient experiments to determine the stress-related concentrations of nZnO and nTiO. Coral polyp retraction, a sublethal effect, was used to evaluate the toxic concentrations. When the theoretical concentrations of nZnO and $nTiO_2$ reached 0.8 and 30 mg/L respectively, after 48 h of exposure, all coral polyps retracted, thereby confirming toxic effects at these concentrations. The retraction of coral polyps is an abnormal morphology displayed by corals when stimulated by the outside world and can be used to reflect growth inhibition in corals (Aminot et al., 2020; Yuan et al., 2023).

2.3. Measurement of nZnO and $nTiO_2$ in coral tissues and experimental water

Waterpik (Waterpik™, 3–5 kgf cm^{-2}) was used to separate coral tissue and mucus from the skeleton. The coral tissue was separated from the water through sedimentation and filtration. The filtrate contained coral mucus and opaque colloidal substances. The weight of the tissue was quantified before and after filtration using a filter membrane. It was then dried and weighed again to obtain the dry weight. The samples were digested with 30% nitric acid, 5% hydrochloric acid, and 5% hydrofluoric acid and then subjected to pressurized microwave digestion at 120–195 °C for 3 h. After digestion, the samples were diluted and analyzed using ICP-MS following the procedures outlined by Jovanovic and Guzman (2014) and Gondikas et al. (2014). The Zn and Ti ion contents were calculated based on the dry weight of the tissue (Han et al., 2020; Zhang et al., 2019).

During the exposure experiment, to detect the contents of ZnO and TiO_2, 1 mL of experimental water was collected at 0, 2, 6, 12, 24, and 48

h after exposure. Then, 30% nitric acid, 5% hydrochloric acid and 5% hydrofluoric acid were added to the samples. Subsequently, the samples were transferred to digestion tubes and placed in a microwave oven for digestion at 148 °C for 2 h. After digestion, the samples were diluted and analyzed by ICP-MS following the procedures outlined by Jovanovic and Guzman (2014) and Gondikas et al. (2014). The Zn and Ti ion concentrations were detected on the instrument, and the oxide concentrations were calculated.

2.4. Density determination of symbiotic zooxanthellae

The density of symbiotic zooxanthellae was measured after exposure to nZnO and $nTiO_2$ using a method described by Tang et al. (2018) and Qin et al. (2019). First, seawater was filtered to collect coral tissues using a 0.45 μm pore size filter. The initial volume of the tissue homogenate was measured in a graduated cylinder and 2 mL was centrifuged to separate the supernatant for further analysis of enzyme activity and reactive oxygen species (ROS) content. The symbiotic zooxanthellae were resuspended and then counted using a hemocytometer. Zooxanthellae density (ZD) was calculated by averaging the hemocytometer counts (n = 8–14); the surface area was determined based on the weight of the aluminum foil used to represent the coral nubbins; and the symbiotic zooxanthellae count per unit surface area was calculated as cells per cm^{-2}.

2.5. Measurement of Chl a content and Fv/Fm

Three aliquots of 15 mL each were collected from the remaining slurry to analyze the Chl *a* content. Each aliquot was centrifuged at 4000×*g* for 5 min and the resulting sediment was stored at 4 °C. Subsequently, the sedimented algae were suspended in 100% acetone for 24 h, ruptured, and then re-centrifuged at 4000×*g* for 5 min. Absorbances at 750, 664, 647, and 630 nm were measured using a spectrophotometer (UV-2700, Japan), and the Chl *a* content was calculated using the equations formulated by Huang et al. (2022).

The maximum quantum yield (*Fv/Fm*) of photosystem II (PS II) of the coral symbionts was measured according to the method described by Akther et al. (2020). Briefly, corals were kept in the dark for 30 min prior to conducting measurements using a diving-PAM underwater fluorometer (WalzHeinzGmbH, Effeltrich, Germany).

2.6. Measurement and imaging of the ROS level

According to the manufacturer's recommendations, the intracellular ROS levels were determined using the DCFH-DA fluorescence probe method (Wan et al., 2019; Yin et al., 2010). Briefly, the supernatant of coral tissues was incubated in 10 μL of DCFH-DA (1 mM) for 2 h. During this time, intracellular esterases convert DCFH-DA into 2′,7′-dichlorodihydrofluorescein (H2DCF), which is then converted to fluorescent 2′,7′-dichlorofluorescein (DCF) by intracellular ROS. To quantify the levels of intracellular ROS, the absorbance at 600 nm and relative luciferase activity (RLU), with excitation and emission wavelengths of 485 and 530 nm, respectively, were measured using a Varioskan Lux plate reader (Thermo Scientific, UK).

2.7. Antioxidant and metabolism-related enzyme activity

Coral samples were taken at 0, 6, 12, 24, and 48 h after exposure to detect enzyme activity. The activities of antioxidant enzymes (superoxide dismutase (SOD), catalase (CAT), glutamate dehydrogenase (GDH), and glutamate synthase (GOGAT)) were measured using commercial kits, following the manufacturer's instructions (Nanjing Jiancheng Bioengineering Institute in Nanjing, China). The total enzyme activity was determined, and the total protein concentration in the supernatant was quantified using the bicinchoninic acid method. The enzyme activities were then normalized to U mg^{-1} protein by dividing them by the total protein concentration.

2.8. High-throughput sequencing of G. fascicularis holobiont metatranscriptome

2.8.1. RNA-seq analysis

The coral nubbins were finely ground and combined with 1 mL of TRIzol reagent (Invitrogen). The resulting mixture was centrifuged at 2397×*g* for 5 min at 4 °C to eliminate the coral skeleton. Total RNA was purified according to a previously documented protocol (Cai et al., 2021; Tang et al., 2018), and 9 cDNA libraries were constructed. These transcriptome libraries were sequenced using the Illumina HiSeq 2500 platform at BGI in Shenzhen, China. All the sequencing reads obtained were deposited in the Sequence Read Archive of the National Center for Biotechnology Information (Accession number: PRJNA961310).

2.8.2. Transcriptome assembly and separation of coral versus symbiont transcripts

Following our previous study, raw reads were filtered and high-quality reads retained (Huang et al., 2022). The resulting clean reads from each library were combined to assemble the transcripts using Trinity software. The transcripts corresponding to the coral host and symbiotic zooxanthellae were separated using BLAST. Raw data were compared with the *G. fascicularis* host genome. The remaining data were compared to the zooxanthellae *Symbiodinium minutum* and *Symbiodinium kawagutii* C1 (available at www.gfas@reefgenomics: genome of *Galaxea fascicularis*). DEGs were identified by comparing them to the untreated control, with a significance threshold of Q-value (Adjusted *P-value*) less than or equal to 0.05 (Aranda et al., 2011; Love et al., 2014).

2.8.3. Transcript profiles and annotation

The internationally recognized gene ontology (GO) classification system (www.geneontology.org) was used. The Kyoto Encyclopedia of Genes and Genomes (KEGG) database, accessible at www.kegg.jp, was utilized to determine the high-level biological system functions and processes (Kanehisa et al., 2008). We identified significantly enriched metabolic or signaling pathways that were abundant in genes using KEGG pathway analysis and compared the results with a reference gene background using a hypergeometric test.

2.9. Quantitative real-time PCR (qRT-PCR) validation of mRNA expression patterns

To confirm the accuracy of the transcriptome data, 12 randomly selected DEGs were validated using quantitative real-time PCR (qRT-PCR), with three replicates for each group. The primers used in this study are listed in Table S1. The expression level of candidate genes was analyzed using the $2^{-\Delta\Delta Ct}$ calculation method and reported as mean ± standard error. qRT-PCR was performed using SYBR premix ExTaq (Takara Bio Inc., Kusatsu, Japan) on a QuantStudio™ Plus fluorescence qPCR instrument, and the gene *Gadph* was used as an internal control.

2.10. Statistical analysis

Data were presented as mean ± standard deviation (SD). Prior to analysis, the assumptions of normality and homogeneity of variances were verified using the Shapiro–Wilk test and Levene's test, respectively. Independent sample t-tests were employed to assess the statistical differences in *Fv/Fm*, Chl *a*, and ZD between the experimental and control groups. Differences in physiological parameters (antioxidant enzyme activities) were determined by one-way analysis of variance (ANOVA). A threshold of $P < 0.05$ was set to determine statistical significance.

3. Results

3.1. Characterization of nZnO and $nTiO_2$

The morphology of nZnO and $nTiO_2$ was determined using SEM. $nTiO_2$ was spherical with a size of approximately 40–60 nm, whereas nZnO was packaged in short rods of approximately 20–40 nm (Fig. S1). nZnO and $nTiO_2$ displayed a slight negative charge with zeta potentials of -38.28 ± 0.08 and -38.44 ± 0.15 mV, respectively (Table S2). The hydrodynamic diameters of nZnO and $nTiO_2$ in water were 1783.53 ± 56.53 and 287.37 ± 9.35 nm, respectively (Table S3).

3.2. Phenotypic and physiological changes in G. fascicularis after nZnO and $nTiO_2$ exposure

Through concentration grading experiments, we found that exceeding 0.8 mg/L nZnO and 30 mg/L $nTiO_2$ could cause coral polyp retraction (Table S4). Therefore, subsequent experiments were conducted using these concentrations. The polyps of *G. fascicularis* retracted significantly after exposure to nZnO and $nTiO_2$, respectively (Fig. 1). Furthermore, the *Fv/Fm*, ZD, and Chl *a* contents of *G. fascicularis* were evaluated after exposure to nZnO and $nTiO_2$ for 48 h (Fig. 2). Compared with the control group (CK), significant decreases in the *Fv/Fm*, ZD, and Chl *a* content of 28.46, 22.97, and 25.88%, respectively, were noted after exposure to nZnO and similar changes were observed after exposure to TiO_2 for 48 h.

3.3. nZnO and $nTiO_2$ concentrations in water and coral tissues

The actual concentrations of nZnO and $nTiO_2$ in the experimental water vary over time (0, 2, 6, 12, 24, and 48 h) and are shown in Fig. 3A and B. Due to the potential sedimentation of nanoparticles in water, the concentrations of nZnO and $nTiO_2$ measured in the aqueous phase decreased gradually with increased exposure time. After a 48-h exposure period, the actual concentrations in the water were determined to be 628 μg/L for nZnO and 1.65 mg/L for $nTiO_2$, representing reductions of 21.87 and 94.51% from their initial concentrations, respectively.

Compared with CK, the levels of Zn and Ti ions in the coral tissue of *G. fascicularis* significantly increased ($P < 0.05$) after exposure nZnO and $nTiO_2$ (Fig. 3C). The quantity of Zn ions was approximately 38 times that of the CK (67.18 versus 1.78 μg/g), and the Ti ion concentration was 24.87 μg/g when compared to 0.43 μg/g for CK. Therefore, the amount of Ti ions accumulated in the tissue of *G. fascicularis* was approximately 1.5 times higher than that of Zn ions.

3.4. Immunofluorescence staining and activity measurement of ROS in coral polyps

Fluorescence staining was used to show the expression and distribution of ROS in coral polyps and examine the impact of nZnO and $nTiO_2$ on oxidative stress (Fig. 4), and a ROS assay kit was used to measure the ROS content at various exposure times (Fig. S2A). Dihydroethidium can enter living cells freely and is oxidized by ROS to form oxyethidium, and ingested oxides can mix with chromosomal DNA to produce red fluorescence. Both nZnO and $nTiO_2$ caused a rapid increase in coral ROS levels, reaching a maximum value of 12–24 h after exposure and then decreasing with exposure time. Compared with $nTiO_2$, exposure to nZnO resulted in higher ROS production in corals.

3.5. Oxidative stress and metabolism-related enzyme activity after nZnO and $nTiO_2$ exposure

After exposure to nZnO or $nTiO_2$, the SOD activity in coral gradually increased with exposure time and reached maximum values of 157.36 and 145.40 U/mg prot, respectively, after 48 h. Compared with exposure to $nTiO_2$, nZnO caused greater SOD activity in corals. Following

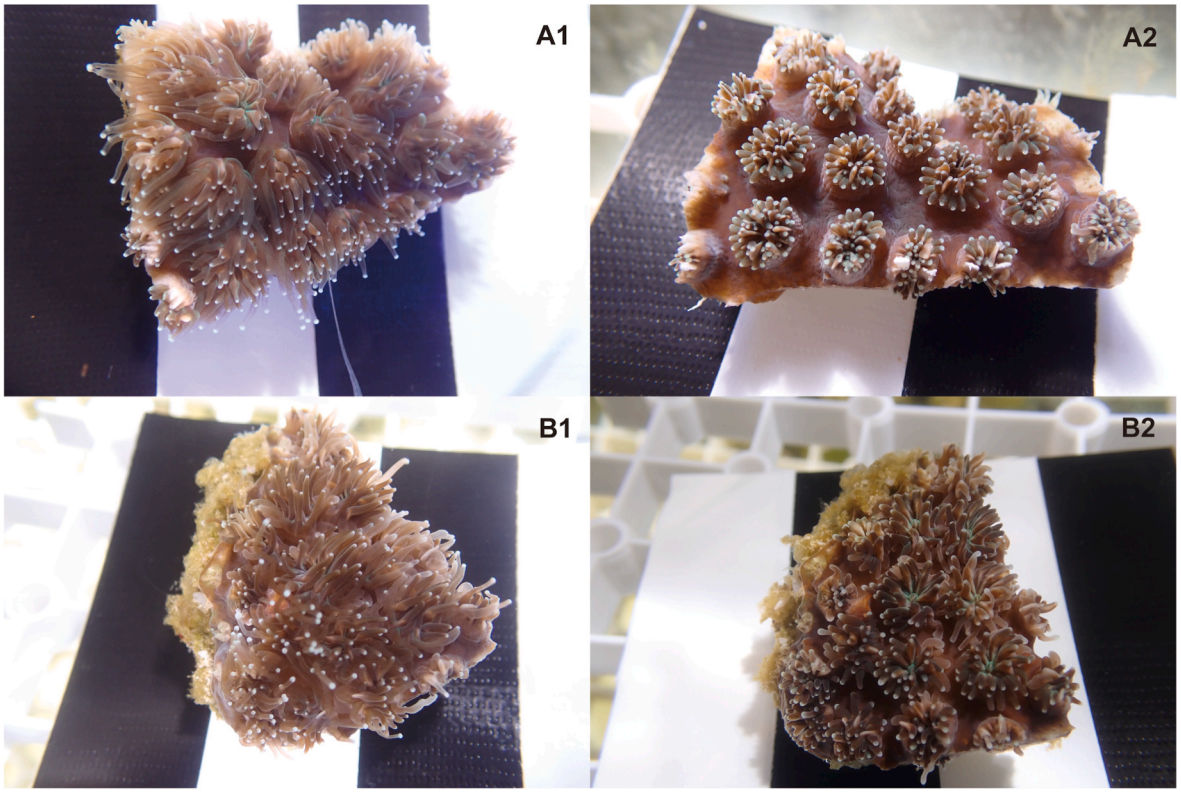

Fig. 1. Coral morphology after $nTiO_2$ and nZnO exposure: A1 and A2 indicate before and after TiO_2 exposure, respectively; B1 and B2 represent before and after exposure to ZnO, respectively.

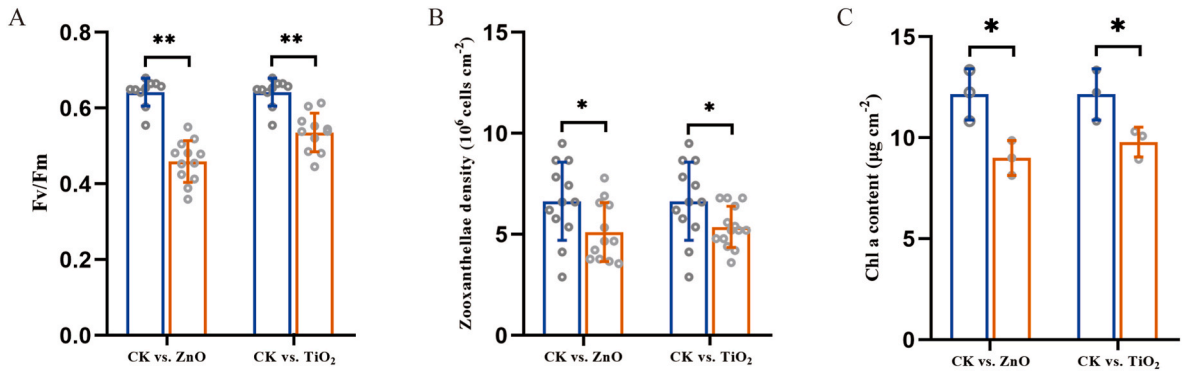

Fig. 2. *Fv/Fm*, density of symbiotic zooxanthellae, and chlorophyll *a* concentrations of *G. fascicularis*. Note: $^*P < 0.05$, $^{**}P < 0.01$.

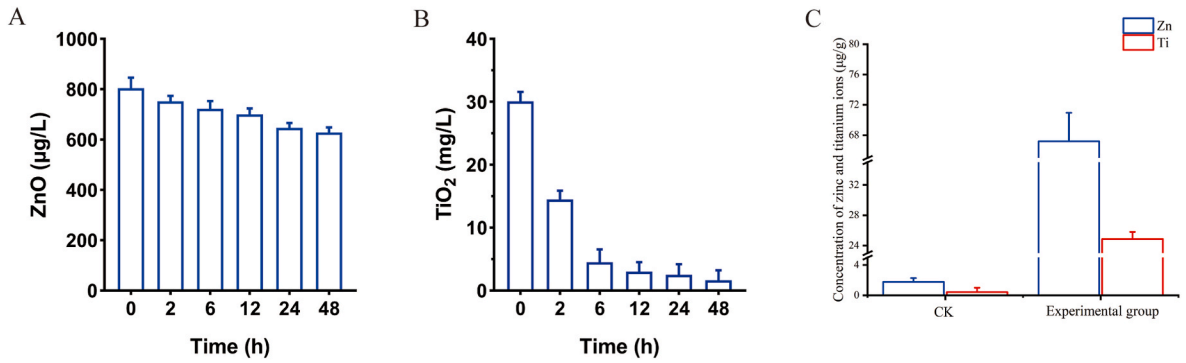

Fig. 3. ZnO and TiO_2 concentrations in water and coral tissues: A and B represent the actual concentration of nZnO and $nTiO_2$ in the experimental water. C represents the accumulation of Zn and Ti in coral tissue.

exposure to nZnO and $nTiO_2$, CAT activity first showed an increasing and then decreasing trend, reaching peak levels of 21.06 and 14.51 U/mg prot, respectively, at 12 h. However, the activities of GDH and GOGAT decreased with increasing exposure time (Figs. S2B–E).

3.6. Transcriptomic responses of *G. fascicularis* to nZnO and $nTiO_2$ exposure

Transcriptomic analysis was carried out after cultivation to explore the mechanisms behind the physiological response of *G. fascicularis*. At this point, 9 cDNA libraries were constructed and sequenced using the DNBSEQ platform. Briefly, we obtained 387.30 million clean counts, with 95.43% of raw reads from nine host samples, with a Q20 value of over 97.54% and GC content ranging from 43.92 to 48.07%. The host mapping rates ranged from 40.22 to 52.42% (Table S5). Principal component analysis (PCA) and correlation analyses showed that both nZnO and $nTiO_2$ treatments profoundly influenced the transcriptome of *G. fascicularis* (Figs. S3 and S4). RNA-seq identified 1888 DEGs in corals following nZnO exposure, including 789 upregulated and 1099 downregulated DEGs. A total of 462 DEGs were identified in corals after $nTiO_2$ exposure, including 202 upregulated and 260 downregulated DEGs, as depicted in the CK volcano plot (Fig. 5A and B). In the comparison between CK and ZnO, 1697 DEGs were found that specifically reacted to ZnO stress. In the comparison between CK and TiO_2, 271 specific DEGs were identified that specifically responded to TiO_2 stress. A total of 191 DEGs were discovered when comparing CK vs. ZnO and CK vs. TiO_2; these represented genes that responded to both stressors. Compared to CK, the number of DEGs in corals exposed to nZnO was significantly greater than that in corals exposed to $nTiO_2$ (Fig. 5C and D).

3.7. GO enrichment analysis of DEGs

The DEGs were categorized into three major Gene Ontology categories: cellular component, biological process, and molecular function. In the comparison between ZnO and CK, the top three terms with the most enriched genes were as follows: cellular anatomical entity, binding, and catalytic activity, which were similar for TiO_2 and CK (Fig. S5). A GO enrichment analysis of the DEGs was conducted to examine their biological significance. In the nZnO group, upregulated DEGs were significantly involved in the regulation of immune system processes (GO: 0002682), immune response (GO: 0006955), regulation of immune response (GO: 0050776), and immune system processes (GO: 0002376), and downregulated DEGs were involved in the extracellular matrix structural constituent GO:0005201 and extracellular region GO:0005576. However, in the $nTiO_2$ group, upregulated DEGs were significantly associated with active transmembrane transporter activity (GO: 0015291), symporter activity (GO: 0015293), and transporter activity (GO: 0005215), and downregulated DEGs were involved in oxidoreductase activity (GO: 0016491), generation of precursor metabolites, and energy (GO: 0006091) (Fig. 6 and Table S6).

3.8. Transcriptomic responses of symbiotic Symbiodiniaceae to nZnO and $nTiO_2$ exposure

In the coral symbiotic *Symbiodiniaceae*, we constructed 9 cDNA libraries yielding 387.3 million high-quality reads, with a Q30 value of over 91.53% and a clean reads ratio between 94.03 and 96.53%. The mapping rates for zooxanthellae C1 varied from 12.40 to 23.36%. Count the number of original sequencing sequences obtained from each sample and the number of sequences obtained after quality control (Table S7). After expression analysis, 0 and 5 differentially expressed symbiont genes were identified in ZnO vs. CK and TiO_2 vs. CK, respectively

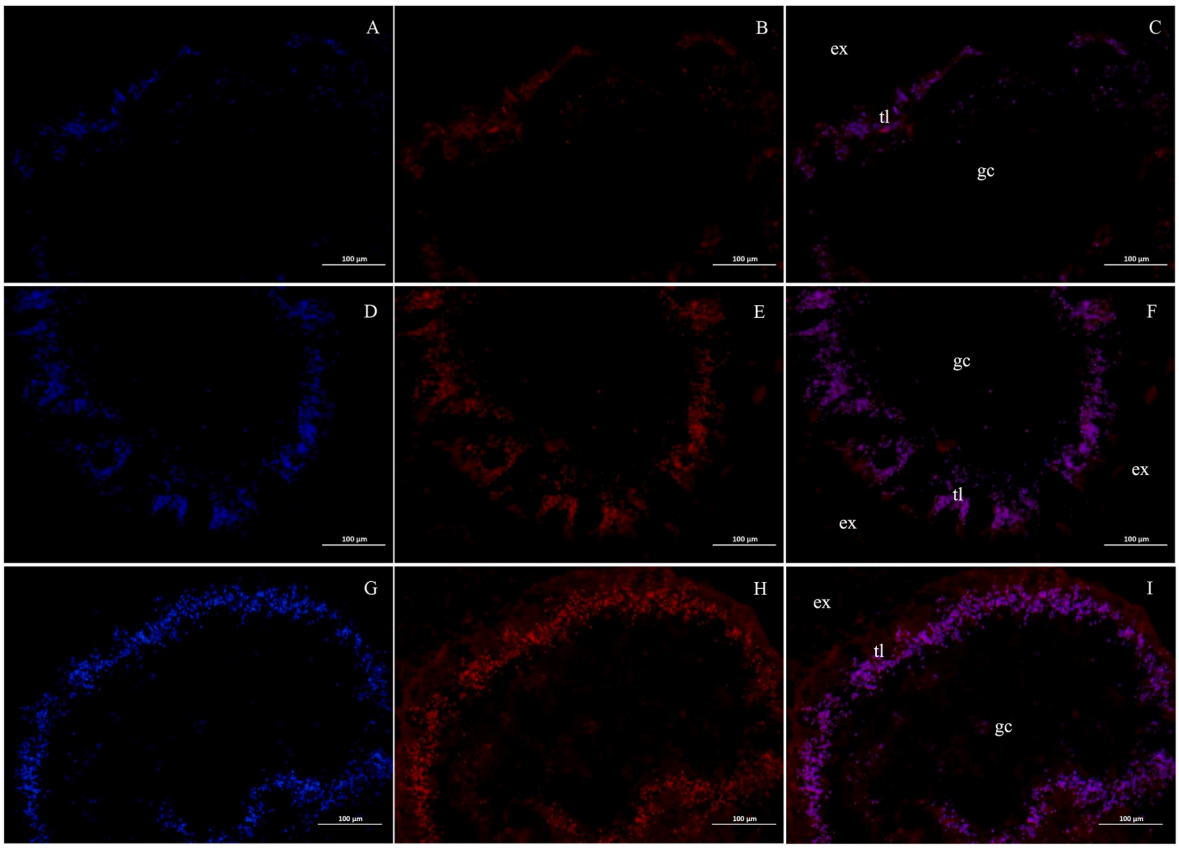

Fig. 4. ROS immunofluorescence staining images of cross-sections of coral tentacles. Dihydroethidium (DHE) can enter cells freely through living cells and undergo oxidation by ROS in cells to form oxyethidium; ingot oxide can be mixed into chromosome DNA to produce red fluorescence.
The amount and changes in ROS content within cells can be assessed based on the intensity of the red fluorescence. Panels A, B, and C represent the control group (CK), while panels D, E, and F represent the $nTiO_2$ exposure group, and panels G, H, and I represent the nZnO exposure group. "ex" denotes the external environment, "tl" denotes the tissue layers, and "gc" denotes the gastric cavity. (For interpretation of the references to color in this figure legend, the reader is referred to the Web version of this article.)

(Table S8). GO enrichment analyses of the DEGs revealed that they were involved in cytoskeleton, zinc ion binding, and transition metal ion binding after $nTiO_2$ exposure (Fig. S6).

3.9. Identification of DEGs related to ROS, immune, and energy metabolism

The DEGs involved in ROS production were analyzed. We screened genes participating in ROS including glutathione S-transferase (*GST*), *SOD*, catalase (*CAT*), glutathione peroxidase (*GPX*), glutaredoxin (*GLX*), thioredoxin (*TRXA*), and serum paraoxonase/arylesterase (*PON*) genes. We identified the DEGs in *G. fascicularis* that are pivotal to energy metabolism, including pyruvate carboxylase (*PC*), glyceraldehyde 3-phosphate dehydrogenase (*GAPDH*), malate dehydrogenase (*MDH*), enolase (*ENO*), and phosphoenolpyruvate carboxykinase (*PEPCK*). Furthermore, in the nZnO group, we observed a significant upregulation of DEGs associated with immune system processes, including toll-like receptors (*TLRs*), mucin-5ac-like (*MUC5AC*), mucin-5B (*MUC5B*), myeloid differentiation primary response protein (*MYD88*), toll-like receptor 2 (*TLR2*), and complement C2-like (*C2*) (Table S9 and Fig. S7). A heat map of these genes, representing their transcriptional levels, was constructed by FPKM values of the samples (Fig. 7A). The PPI (Protein-Protein Interaction) network results showed that *GPX* and *ENO* genes had the highest betweenness centrality, indicating that they had the strongest relationship with other genes (Fig. 7B and C).

3.10. Validation of gene expression patterns using qRT-PCR

The expression levels of the 12 genes were validated using qRT-PCR. The results showed that the expression patterns obtained from qRT-PCR and RNA-Seq were largely consistent. The expression levels of the genes often showed either an upward trend followed by a downward trend or vice versa (Fig. 8). Discrepancies in expression levels can be attributed to the distinct calculation methods of qRT-PCR and RNA-Seq. This concordance substantiates the fidelity of the transcriptomic profiles.

4. Discussion

4.1. Impact of inorganic UVF bio-concentration on coral health

Upon exposure to different concentrations of nZnO and $nTiO_2$, coral polyp retraction appeared to be distinctly dose-dependent. All polyps retracted with nZnO and $nTiO_2$ concentrations of 0.8 and 30 mg/L, respectively. Upon initial exposure to UV filters, we observed a consistent and reproducible polyp retraction response, indicating a reliable biological reaction to these substances. The uniformity of this response across individuals suggests a common sensitivity to the presence of UV filters, highlighting the potential for this reaction as a bioindicator of exposure. Polyp retraction is a direct and rapid physiological response of corals to environmental stress and toxicant exposure and is also a sub-lethal effect of coral exposure to pollutants (He et al., 2019; Stien et al., 2019). Polyp retraction is an intuitive behavioral manifestation of corals in response to environmental stress, and its mechanism is related to physiological regulation. When corals are exposed to pollutants, they

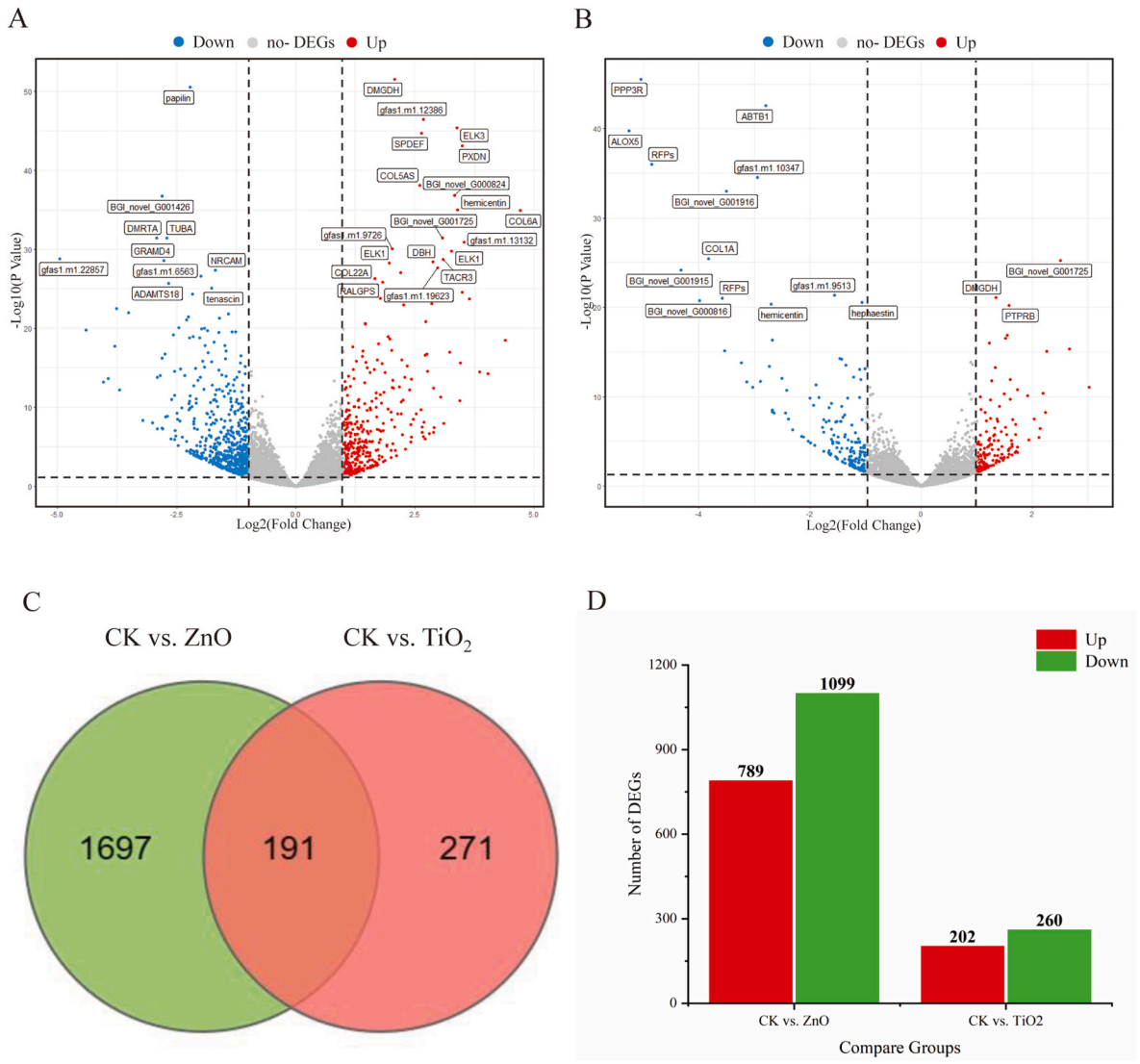

Fig. 5. Analyses of differentially expressed genes (DEGs) in *G. fascicularis* after nZnO and $nTiO_2$ exposure: A and B represent the volcano plots of DEGs after ZnO and TiO_2 exposure, respectively. Genes with -log10(*P*-value)≥20 are labeled with gene names in the figure. C and D represent the number of DEGs in *G. fascicularis* exposed to CK vs. ZnO and CK vs. TiO_2 groups, respectively.

close their gastrodermal cavity through polyp retraction; this may be a self-protection method to reduce or delay the toxic effects (May et al., 2020). Different sunscreen components (BP-1, BP-3, BP-4, and BP-8) cause different levels of coral polyp retraction, indicating that corals have different sensitivities to different UVFs (He et al., 2019). Polyp retraction upon exposure to nZnO and $nTiO_2$ in this study indicated that these components exerted stress on coral growth.

Upon exposure to nZnO and $nTiO_2$, the concentrations of Zn and Ti in coral tissues increased by 38 and 58 times, respectively; this may have been due to the capture of nZnO and $nTiO_2$ particles by *G. fascicularis* and their accumulation in coral tissues. A recent study also observed ZnO and TiO_2 particles from physical sunscreen in the tissues of button corals and detected Zn and Ti at concentrations reaching 327.4 and 701.3 μg/g DW in the tissues (Yuan et al., 2023). This study found high ROS concentrations in coral tissues (Fig. 4 and Fig. S2A). nZnO and $nTiO_2$ in 1 g of sunscreen can generate up to 463 Nm/h of hydrogen peroxide in seawater, and nZnO and $nTiO_2$ are the primary oxidants entering coastal waters, directly impacting the ecosystem (Sanchez-Quiles and Tovar-Sanchez, 2014). This indicates that the excessive ROS in coral tissues may be generated due to the entry of nZnO and $nTiO_2$ into coral tissues. ROS are highly reactive substances that play a crucial role in the oxidative stress process and are regarded as the engines of the oxidative stress response (Matyas et al., 2021). An increase in ROS concentration can lead to cell wall or cell damage, lipid peroxidation, and growth inhibition, thereby harming organisms (Jovanovic and Guzman, 2014; Li et al., 2021; Luo et al., 2020; Schneider and Lim, 2019). In this study, nZnO and $nTiO_2$ bioaccumulated in coral tissues and generated large amounts of ROS, which may have led to a decrease in ZD, Chl *a*, and *Fv/Fm* in relation to the inorganic UVFs. Photosynthetic characteristics, such as ZD, Chl *a*, and *Fv/Fm*, are important autotrophic indices of corals and are crucial indicators for assessing the health of coral symbiosis systems (Pei et al., 2022b; Saskia et al., 2013). The decline in ZD, Chl *a*, and *Fv/Fm* indicates that the enrichment of nZnO and $nTiO_2$ harms corals.

4.2. *nZnO exposure: activating coral immune system and excessively consuming coral physiological functions*

For corals living in tropical waters, the immune response is among the most crucial physiological processes in stress response (Tang et al., 2018). The innate immune system of corals is responsible for maintaining the integrity and stability of the internal environment and is also

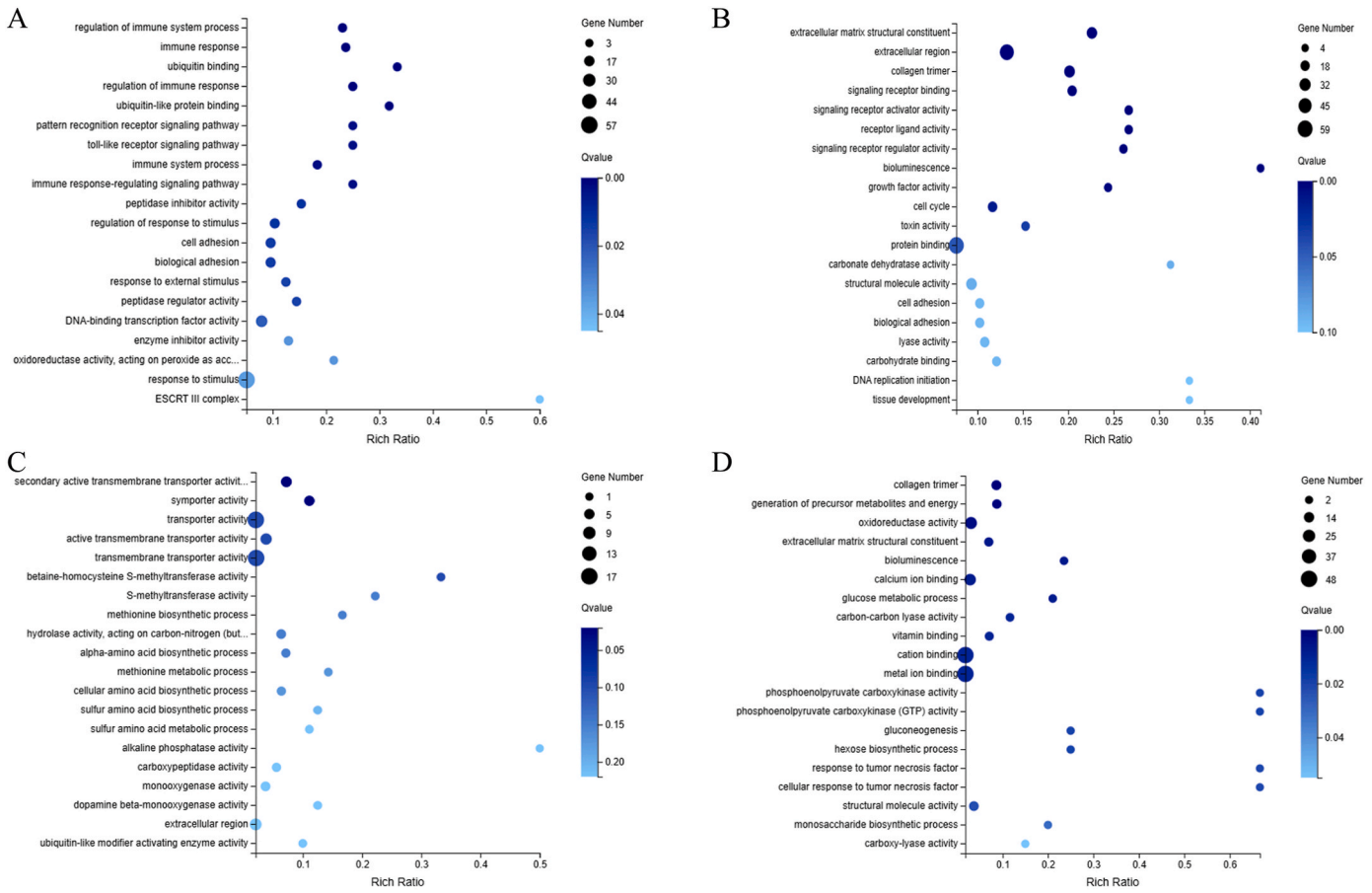

Fig. 6. GO enrichment analysis of up-and down-regulated expressed genes after nZnO and $nTiO_2$ exposure: A and B represent upregulation and downregulation of expression after nZnO exposure, respectively; C and D represent upregulation and downregulation of expression after $nTiO_2$ exposure, respectively.

an important defense mechanism for corals to respond to external pathogens and environmental stress (Mansfield and Gilmore, 2019). The toll-like receptors and complement systems constitute innate defense systems against pathogens. The complement system also recognizes and opsonizes non-self-particles, including nanomaterials and damaged host cells (Chen et al., 2018; Hajishengallis and Lambris, 2010; Wu et al., 2024). In this study, we found that the expression levels of innate immunity-related genes, such as *TLRs*, *MUC5AC*, and *C2*, were significantly upregulated upon exposure to nZnO (Fig. S7). These genes are related to innate immunity factors such as TLR, lectins, and integrins (Palmer and Traylor-Knowles, 2012). Similar findings were reported by Wu et al. (2024). Exposure to nZnO led to upregulated gene expression of the complement system (*C1* and *C3*) and toll-like receptors *TLRb* and *TLRc* in mussels, thereby activating the innate immune response of mussels. In Di et al. (2019), the *MUC5AC* protein identified in *Babylonia areolata* was significantly involved in maintaining the immune homeostasis of invertebrates. Alpha-L-fucosidase (*AFU*) has immunomodulatory effects and is a marker of chronic inflammation. *AFU* cleaves fucose during decomposition and its deficiency can cause pathological reactions (Sobkowicz et al., 2014). Wei et al. (2009) found that *C2* plays a key role in the immune response of fish (*Pseudosciaena crocea*) to bacterial attacks. *TLRs* are key components of the immune system and can induce innate immunity by recognizing pathogen-associated molecular patterns in various microorganisms and activating signaling cascades (Rauta et al., 2014). This indicates that nZnO exposure affects the immune system of reef-building corals and can activate their innate immunity by regulating the expression of TLR, lectins, and integrins. Activation of the coral immune system by nZnO exposure may cause excessive consumption of the physiological functions of corals, impact their normal growth and metabolism, and negatively affect the health status of corals.

4.3. $nTiO_2$ exposure: blocking coral energy supply and increasing nutritional requirements

The transcriptome results showed that the toxicity mechanism of $nTiO_2$ in corals may differ from that of nZnO. Upon $nTiO_2$ exposure, corals contained 462 DEGs, including 202 significantly upregulated genes mainly enriched in transporter activity and 260 significantly downregulated genes mainly enriched in the generation of precursor metabolites and energy (Fig. 6D). Further analysis showed that these downregulated DEGs were related to energy metabolism, such as carbon metabolism, citric acid cycle (TCA), pyruvate metabolism, and glycolysis/gluconeogenesis ($P < 0.05$) (Fig. S8). Some of the genes related to glycolysis/gluconeogenesis, such as glyceraldehyde 3-phosphate dehydrogenase (*GAPDH*), phosphoenolpyruvate carboxykinase (*PEPCK*), enolase (*ENO*), pyruvate carboxylase (*PC*) and TCA, malate dehydrogenase (*MDH*), and succinate dehydrogenase (ubiquinone) cytochrome *b*560 subunit (*SDHC*) were significantly downregulated (Fig. S7).

Upon $nTiO_2$ exposure, some transporter genes in corals, such as monocarboxylate transporter 4-like isoform X1 (*MCT4*) and major facilitator superfamily domain-containing protein (*MFSD2A*), were significantly upregulated (Fig. S7). The transporters encoded by these genes have significant roles in regulating material transportation and cell metabolism. *MCT4* mainly mediates the transmembrane transport of substances such as lactic acid, pyruvate, and ketone bodies (Halestrap and Meredith, 2004). This type of transport is important for cellular energy metabolism and pH regulation (Halestrap and Meredith, 2004;

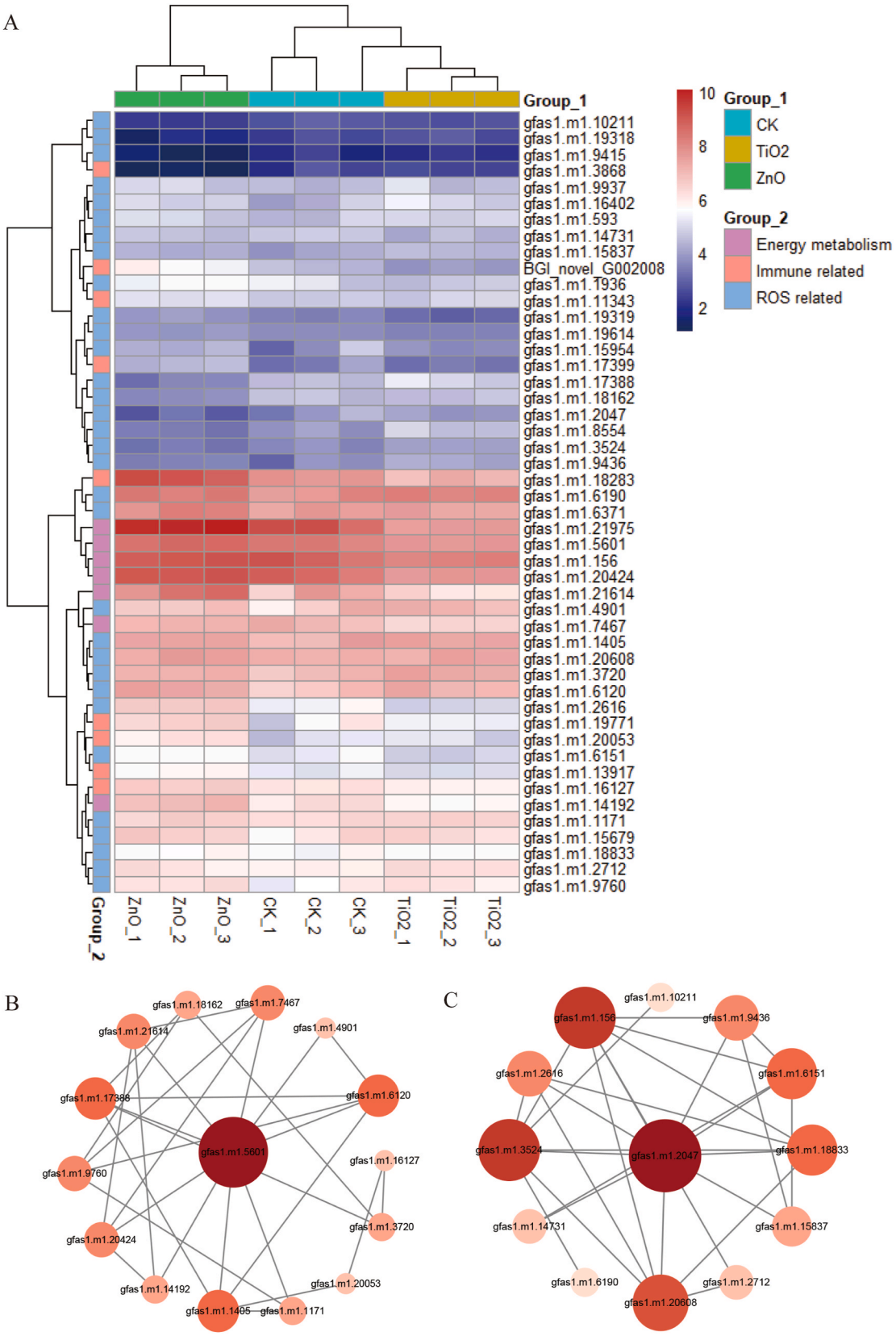

Fig. 7. Differential clustering and PPI network analysis of genes related to ROS, energy metabolism, and immunity.
(A) Heatmap of expression profiles for genes. (B–C) The PPI network of genes. Each dot represents a gene, and the connecting line indicates the interaction between the two genes. The size and color of each point reflect the number of interaction connections: larger points indicate more connections, while the color transitions from white to red, with deeper red indicating a greater number of connections. (For interpretation of the references to color in this figure legend, the reader is referred to the Web version of this article.)

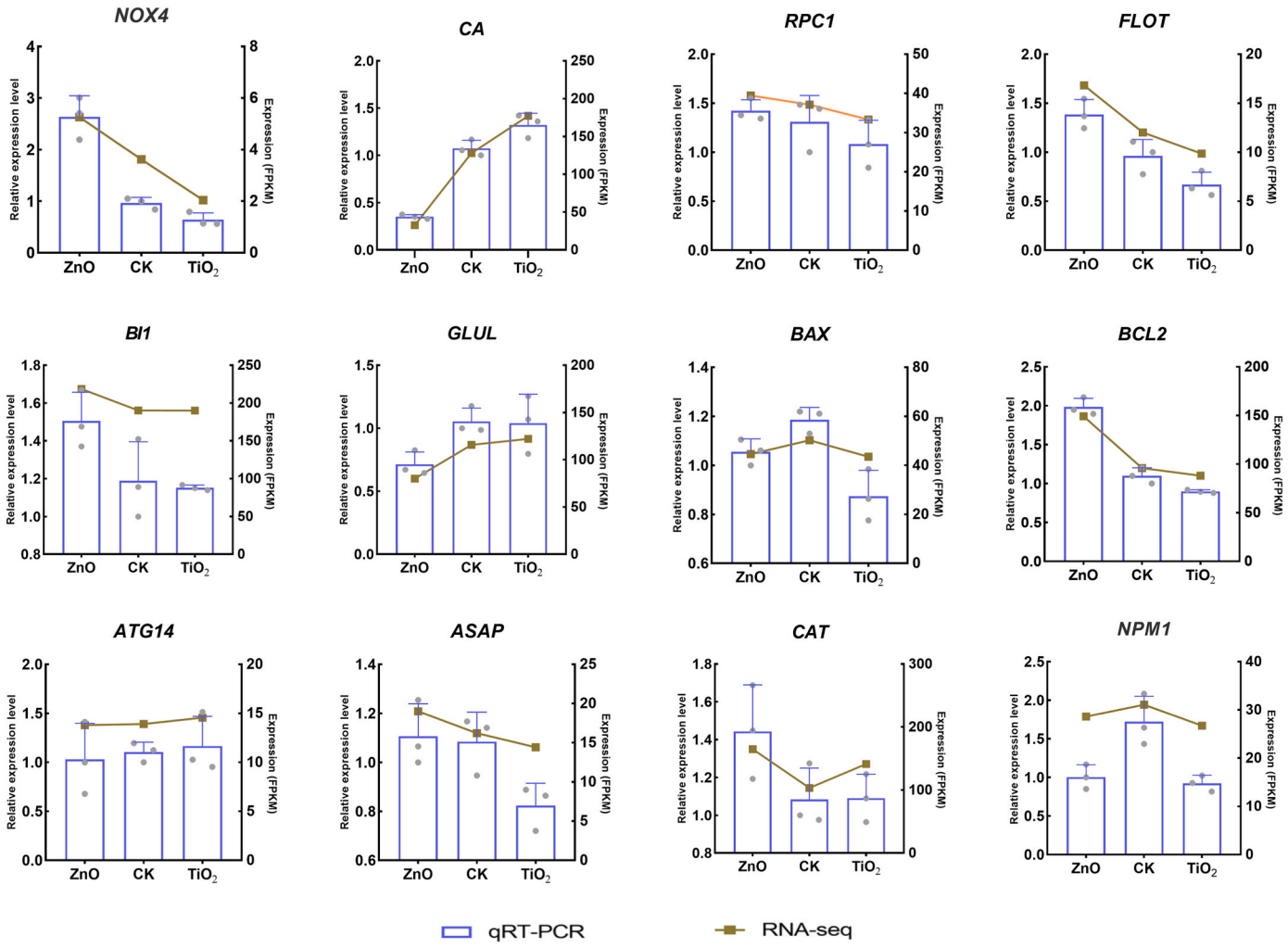

Fig. 8. qRT-PCR analysis of genes for the validation of RNA-Seq data.

Zhang et al., 2021). *MFSD2A* can transport a variety of important metabolism-related substances, such as glucose, fatty acids, pyruvate, and specific amino acids (Berger et al., 2012). In organisms, membrane transporters are highly significant in maintaining the balance inside and outside cells as they can selectively allow small molecules, such as ions and nutrients, to pass through the plasma membrane (Wang et al., 2021). In this study, the upregulated expression of transporter activity genes enhanced the transport ability of transmembrane transport, indicating that nTiO₂ exposure may prompt corals to respond to the pressure of $nTiO_2$ by regulating the expression of these transporter genes to maintain intracellular material balance and normal metabolism.

As key pathways for cells to generate energy (ATP), glucose metabolism and the TCA cycle guarantee the life of organisms and promote normal physiological activities (Kaniewska et al., 2015; Pei et al., 2022a). The enzyme encoded by *GAPDH* plays a key role in glycolysis; it converts glyceraldehyde-3-phosphate into 1,3-bisphosphoglycerate, generating NADH and ATP to provide energy to cells (Molina et al., 2017). *PEPCK* catalyzes the conversion of oxaloacetate to phosphoenolpyruvate during gluconeogenesis (Polato et al., 2010) and can catalyze the reverse reaction as part of the succinate/propionate/acetate pathway to generate anaerobic energy in some facultative anaerobic invertebrates (Bollati et al., 2022). In corals, the transcription level of *PEPCK* changes due to stressful conditions such as high temperatures and bacterial attacks, which affect coral metabolism (Sun et al., 2022; Wright et al., 2017). *PC* catalyzes the conversion of pyruvate into oxaloacetate, and this step occurs directly before the step catalyzed by *PEPCK* during gluconeogenesis. In mammals, *PC* plays a vital role in gluconeogenesis and lipogenesis, the biosynthesis of neurotransmitter substances, and islet glucose-induced insulin secretion (López-Alonso et al., 2022). It is therefore likely that nTiO₂ exposure inhibits the expression of genes related to energy production and material metabolism in corals, which may impact their energy supply and material synthesis, thereby affecting their normal physiological functions and survival ability. Changes in the transcription levels of some transporters reflect the metabolic regulation of corals in adverse environments, such as $nTiO_2$ exposure. In conclusion, $nTiO_2$ disrupts the energy supply of corals, leading to an increased demand for nutrient transport.

4.4. *Comparing toxicity following G. fascicularis exposure to nZnO and nTiO₂*

nZnO and $nTiO_2$ are the major components in many sunscreens. To make sunscreen transparent and more comfortable, ZnO and TiO_2 are usually present in nanoparticles with sizes less than 100 nm (Bocca et al., 2018; Jeon et al., 2016). Non-specific oxidative stress is likely an important factor in the toxicity of nanoparticles (Nel et al., 2006); when organisms are stressed by environmental pollution, the ROS levels in the body increase and excessive ROS disrupts the redox balance, triggers lipid peroxide oxidation and DNA damage, and affects organisms (Zhang et al., 2023). CAT and SOD are important antioxidant defense systems in organisms. They catalyze the generation of H_2O and O_2 from ROS (Asagba et al., 2008; Zhang et al., 2023), and GSH-Px cooperates with

SOD to scavenge free radicals, convert lipid peroxides, and reduce oxidative damage (Lin et al., 2018). In this study, nZnO and $nTiO_2$ exposure significantly increased ROS activity. As the exposure time increased, high concentrations of ROS inhibited CAT activity (Fig. S2), which indicated that nZnO and $nTiO_2$ destroyed the antioxidant defense system of corals.

GOGAT plays a key role in the nitrogen metabolism process. The reduction in its activity may lead to interference in nitrogen assimilation and circulation processes and affect the synthesis of nitrogen-containing compounds, such as amino acids and proteins (Lu et al., 2011). GDH catalyzes the oxidative deamination of glutamic acid to generate α-ketoglutaric acid and ammonia, which is important for regulating the ammonia level and nitrogen metabolism balance in cells (Liu et al., 2024; Ma et al., 2019). In the present study, the activities of GOGAT and GDH were significantly reduced, indicating that nitrogen metabolism in corals was affected upon exposure to the two UVFs. Corals and marine invertebrates can improve their survival ability by slowing down the metabolic rate in response to the pressure caused by seawater warming or acidification (Basile et al., 2005; Yu et al., 2020).

nZnO triggered an innate immune response in corals. The innate immune system plays a crucial role as the first line of defense for organisms to resist the invasion of external pathogens (Diamond and Kanneganti, 2022). Genes related to innate immunity, such as *MASP1, MUC5AC, TLRs*, and *C2*, were significantly upregulated, indicating that after the corals were exposed to nZnO, they could recognize potential threats and quickly activate immune defense mechanisms. This indicates that nZnO is recognized by corals as a similar pathogen or harmful stimulus, triggering an immune response. However, $nTiO_2$ primarily affects the energy supply and demand relationships of corals; this may be due to $nTiO_2$ affecting mitochondrial function or the activity of enzymes related to energy production. An insufficient energy supply affects various physiological activities in corals, including feeding, growth, and maintenance of basic life functions (Beck et al., 2024). The DEGs enriched in the precursor metabolite pathways indicated that $nTiO_2$ interfered with the material metabolism of corals. Therefore, corals may not be able to normally synthesize the required biomolecules, and disorders in material metabolism will further affect the overall health and survival of corals.

nZnO and $nTiO_2$ have different toxicity mechanisms in corals, which is likely due to differences in the chemical properties of the nZnO and $nTiO_2$ particles. Unlike the almost insoluble $nTiO_2$, nZnO can dissolve in water and release zinc ions, leading to its toxicity to aquatic organisms (Ates et al., 2013; Brun et al., 2014; Yuan et al., 2023). Therefore, the ions released after the dissolution of the nZnO and $nTiO_2$ particles may have different toxicity mechanisms in corals. In addition, the shapes and sizes of the nZnO and $nTiO_2$ used in this study differed, with the nZnO particles being dendritic and smaller than the $nTiO_2$ particles (Fig. S1). Such differences in the shapes and sizes of nZnO and $nTiO_2$ may be another reason for different toxicity mechanisms. The smaller the particle size, the greater the potential of penetrating organisms and cells and the greater the toxicity (Ispas et al., 2009; Mironava et al., 2010; Xiong et al., 2011). Dendritic and clustered nanoparticles are known to be more toxic than spherical NPs (Ispas et al., 2009). Therefore, the differences in chemical properties, such as ion release, shape, and size of the nZnO and $nTiO_2$ particles, likely attribute to their different toxicity mechanisms, providing an important clue to understanding the impact of sunscreens on coral ecosystems. Therefore, when evaluating the environmental risks of sunscreens, the specific toxicity mechanisms of different sunscreens must be considered to take targeted protection measures. To better protect the health and stability of coral reef ecosystems, further studies are required to determine the interactions between sunscreens and corals.

5. Conclusion

Our study provides a comparative analysis of the physiological and transcriptomic responses of *G. fascicularis* to inorganic UVFs, nZnO and $nTiO_2$. We observed that nZnO and $nTiO_2$ exert distinct toxic effects on coral health, with nZnO demonstrating a more pronounced impact on the coral immune system and oxidative stress indicators, such as ROS, SOD, and CAT activities. Notably, nZnO upregulated key immune-related genes like *TLRs*, *MUC5AC*, and *C2*, suggesting a direct influence on coral immunity. In contrast, $nTiO_2$ primarily downregulated metabolic genes including *GAPDH*, *PEPCK*, *PC*, *ENO*, and *SDHC*, potentially inhibiting energy metabolism and material synthesis in corals. These findings underscore the differential mechanisms of toxicity and provide a comprehensive reference for assessing the risks of inorganic UVFs to scleractinian corals.

CRediT authorship contribution statement

Jian Chen: Writing – review & editing, Writing – original draft, Investigation, Funding acquisition, Formal analysis, Data curation, Conceptualization. **Kefu Yu:** Writing – review & editing, Supervision, Resources, Funding acquisition, Conceptualization. **Xiaopeng Yu:** Supervision, Software, Methodology, Investigation. **Ruijie Zhang:** Visualization, Validation, Supervision, Project administration. **Biao Chen:** Resources, Methodology, Formal analysis, Data curation.

Funding

The study was funded by the National Natural Science Foundation of China (Nos. 42030502 and 42090041), and the Innovation Project of Guangxi Graduate Education (No. YCBZ2024045).

Declaration of competing interest

The authors declare that they have no known competing financial interests or personal relationships that could have appeared to influence the work reported in this paper.

Appendix A. Supplementary data

Supplementary data to this article can be found online at https://doi.org/10.1016/j.envres.2024.120663.

Data availability statement

The raw reads of the scleractinian coral *G. fascicularis* in this study were submitted to the National Center for Biotechnology Information Sequence Read Archive (accession number: PRJNA961310).

References

Akther, S., Suzuki, J., Pokhrel, P., Okada, T., Imamura, M., Enomoto, T., Kitano, T., Kuwahara, Y., Fujita, M., 2020. Behavior of eukaryotic symbionts in large benthic foraminifers *Calcarina gaudichaudii* and *Baculogypsina sphaerulata* under exposure to wastewater. Environ. Pollut. 265, 114971. https://doi.org/10.1016/j.envpol.2020.114971.

Aminot, Y., Lanctôt, C., Bednarz, V., Robson, W.J., Taylor, A., Ferrier-Pagès, C., Metian, M., Tolosa, I., 2020. Leaching of flame-retardants from polystyrene debris: bioaccumulation and potential effects on coral. Mar. Pollut. Bull. 151, 110862. https://doi.org/10.1016/j.marpolbul.2019.110862.

Aranda, M., Banaszak, A.T., Bayer, T., Luyten, J.R., Medina, M., Voolstra, C.R., 2011. Differential sensitivity of coral larvae to natural levels of ultraviolet radiation during the onset of larval competence. Mol. Ecol. 20 (14), 2955–2972. https://doi.org/10.1111/j.1365-294X.2011.05153.x.

Asagba, S.O., Eriyamremu, G.E., Igberaese, M.E., 2008. Bioaccumulation of cadmium and its biochemical effect on selected tissues of the catfish (*Clarias gariepinus*). Fish Physiol. Biochem. 34 (1), 61–69. https://doi.org/10.1007/s10695-007-9147-4.

Ates, M., Daniels, J., Arslan, Z., Farah, I.O., Rivera, H.F., 2013. Comparative evaluation of impact of Zn and ZnO nanoparticles on brine shrimp (*Artemia salina*) larvae: effects of particle size and solubility on toxicity. Environ. Sci. Process. Impacts. 15 (1), 225–233. https://doi.org/10.1039/c2em30540b.

Basile, M., Christos, O., Andreas, P., Hans, O.P.Â.r., 2005. Effects of long-term moderate hypercapnia on acid-base balance and growth rate in marine mussels *Mytilus*

galloprovincialis. Mar. Ecol.: Prog. Ser. 293, 109–118. https://doi.org/10.3354/meps293109.

BBC, 2018. Coral: Palau to ban sunscreen products to protect reefs. https://www.bbc.com/news/science-environment-46046.

Beck, K.K., Schmidt-Grieb, G.M., Kayser, A.S., Wendels, J., Kler Lago, A., Meyer, S., Laudien, J., Häussermann, V., Richter, C., Wall, M., 2024. Cold-water coral energy reserves and calcification in contrasting fjord environments. Sci. Rep. 14 (1), 5649. https://doi.org/10.1038/s41598-024-56280-2.

Berger, J.H., Charron, M.J., Silver, D.L., 2012. Major facilitator superfamily domain-containing protein 2a (*MFSD2A*) has roles in body growth, motor function, and lipid metabolism. PLoS One 7 (11), e50629. https://doi.org/10.1371/journal.pone.0050629.

Bocca, B., Caimi, S., Senofonte, O., Alimonti, A., Petrucci, F., 2018. ICP-MS based methods to characterize nanoparticles of TiO_2 and ZnO in sunscreens with focus on regulatory and safety issues. Sci. Total Environ. 630, 922–930. https://doi.org/10.1016/j.scitotenv.2018.02.166.

Bollati, E., Rosenberg, Y., Simon-Blecher, N., Tamir, R., Levy, O., Huang, D., 2022. Untangling the molecular basis of coral response to sedimentation. Mol. Ecol. 31 (3), 884–901. https://doi.org/10.1111/mec.16263.

Brun, N.R., Lenz, M., Wehrli, B., Fent, K., 2014. Comparative effects of zinc oxide nanoparticles and dissolved zinc on zebrafish embryos and eleuthero-embryos: importance of zinc ions. Sci. Total Environ. 476–477, 657–666. https://doi.org/10.1016/j.scitotenv.2014.01.053.

Cai, S., Wang, H., Tang, J., Tang, X., Guan, P., Li, J., Jiang, Y., Wu, Y., Xu, R., 2021. Feedback mechanisms of periphytic biofilms to ZnO nanoparticles toxicity at different phosphorus levels. J. Hazard Mater. 416, 125834. https://doi.org/10.1016/j.jhazmat.2021.125834.

Chen, Y., Xu, K., Li, J., Wang, X., Ye, Y., Qi, P., 2018. Molecular characterization of complement component 3 (*C3*) in Mytilus coruscus improves our understanding of bivalve complement system. Fish Shellfish Immunol. 76, 41–47. https://doi.org/10.1016/j.fsi.2018.02.044.

Cunningham, B., Torres-Duarte, C., Cherr, G., Adams, N., 2020. Effects of three zinc-containing sunscreens on development of purple sea urchin (*Strongylocentrotus purpuratus*) embryos. Aquat. Toxicol. 218, 105355. https://doi.org/10.1016/j.aquatox.2019.105355.

Di, G., Li, Y., Zhao, X., Wang, N., Fu, J., Li, M., Huang, M., You, W., Kong, X., Ke, C., 2019. Differential proteomic profiles and characterizations between hyalinocytes and granulocytes in ivory shell *Babylonia areolata*. Fish Shellfish Immunol. 92, 405–420. https://doi.org/10.1016/j.fsi.2019.06.036.

Diamond, M.S., Kanneganti, T.-D., 2022. Innate immunity: the first line of defense against SARS-CoV-2. Nat. Immunol. 23 (2), 165–176. https://doi.org/10.1038/s41590-021-01091-0.

Downs, C.A., Diaz-Cruz, M.S., White, W.T., Rice, M., Jim, L., Punihaole, C., Dant, M., Gautam, K., Woodley, C.M., Walsh, K.O., Perry, J., Downs, E.M., Bishop, L., Garg, A., King, K., Paltin, T., McKinley, E.B., Beers, A.I., Anbumani, S., Bagshaw, J., 2022. Beach showers as sources of contamination for sunscreen pollution in marine protected areas and areas of intensive beach tourism in Hawaii, USA. J. Hazard Mater. 438, 129546. https://doi.org/10.1016/j.jhazmat.2022.129546.

Downs, C.A., DiNardo, J.C., Stien, D., Rodrigues, A.M.S., Lebaron, P., 2021. Benzophenone accumulates over time from the degradation of octocrylene in commercial sunscreen products. Chem. Res. Toxicol. 34 (4), 1046–1054. https://doi.org/10.1021/acs.chemrestox.0c00461.

Downs, C.A., Kramarsky-Winter, E., Segal, R., Fauth, J., Knutson, S., Bronstein, O., Ciner, F.R., Jeger, R., Lichtenfeld, Y., Woodley, C.M., Pennington, P., Cadenas, K., Kushmaro, A., Loya, Y., 2016. Toxicopathological effects of the sunscreen UV filter, oxybenzone (benzophenone-3), on coral planulae and cultured primary cells and its environmental contamination in Hawaii and the US Virgin Islands. Arch. Environ. Contam. Toxicol. 70 (2), 265–288. https://doi.org/10.1007/s00244-015-0227-7.

Downs, C.A., Woodley, C.M., Fauth, J.E., Knutson, S., Burtscher, M.M., May, L.A., Avadanei, A.R., Higgins, J.L., Ostrander, G.K., 2011. A survey of environmental pollutants and cellular-stress markers of Porites astreoides at six sites in St. John, U. S. Virgin Islands. Ecotoxicology 20 (8), 1914–1931. https://doi.org/10.1007/s10646-011-0729-7.

Glaesser, D., Kester, J., Paulose, H., Alizadeh, A., Valentin, B., 2017. Global travel patterns: an overview. J. Trav. Med. 24 (4). https://doi.org/10.1093/jtm/tax007.

Gondikas, A.P., von der Kammer, F., Reed, R.B., Wagner, S., Ranville, J.F., Hofmann, T., 2014. Release of TiO_2 nanoparticles from sunscreens into surface waters: a one-year survey at the old Danube recreational Lake. Environ. Sci. Technol. 48 (10), 5415–5422. https://doi.org/10.1021/es405596y.

Hajishengallis, G., Lambris, J.D., 2010. Crosstalk pathways between Toll-like receptors and the complement system. Trends Immunol. 31 (4), 154–163. https://doi.org/10.1016/j.it.2010.01.002.

Halestrap, A.P., Meredith, D., 2004. The SLC16 gene family-from monocarboxylate transporters (MCTs) to aromatic amino acid transporters and beyond. Pflugers Arch-Eur. J. Physiol. 447 (5), 619–628. https://doi.org/10.1007/s00424-003-1067-2.

Han, M., Zhang, R., Yu, K., Li, A., Wang, Y., Huang, X., 2020. Polycyclic aromatic hydrocarbons (PAHs) in corals of the South China Sea: occurrence, distribution, bioaccumulation, and considerable role of coral mucus. J. Hazard Mater. 384, 121299. https://doi.org/10.1016/j.jhazmat.2019.121299.

He, T., Tsui, M.M.P., Mayfield, A.B., Liu, P.J., Chen, T.H., Wang, L.H., Fan, T.Y., Lam, P. K.S., Murphy, M.B., 2023. Organic ultraviolet filter mixture promotes bleaching of reef corals upon the threat of elevated seawater temperature. Sci. Total Environ. 876, 162744. https://doi.org/10.1016/j.scitotenv.2023.162744.

He, T., Tsui, M.M.P., Tan, C.J., Ng, K.Y., Guo, F.W., Wang, L.H., Chen, T.H., Fan, T.Y., Lam, P.K.S., Murphy, M.B., 2019. Comparative toxicities of four benzophenone ultraviolet filters to two life stages of two coral species. Sci. Total Environ. 651, 2391–2399. https://doi.org/10.1016/j.scitotenv.2018.10.148.

Huang, W., Yang, E., Yu, K., Meng, L., Wang, Y., Liang, J., Huang, X., Wang, G., 2022. Lower cold tolerance of tropical *Porites lutea* is possibly detrimental to its migration to relatively high latitude refuges in the South China Sea. Mol. Ecol. https://doi.org/10.1111/mec.16662.

Ispas, C., Andreescu, D., Patel, A., Goia, D.V., Andreescu, S., Wallace, K.N., 2009. Toxicity and developmental defects of different sizes and shape nickel nanoparticles in zebrafish. Environ. Sci. Technol. 43 (16), 6349–6356. https://doi.org/10.1021/es9010543.

Jeon, S.K., Kim, E.J., Lee, J., Lee, S., 2016. Potential risks of TiO_2 and ZnO nanoparticles released from sunscreens into outdoor swimming pools. J. Hazard Mater. 317, 312–318. https://doi.org/10.1016/j.jhazmat.2016.05.099.

Jiang, D., Yang, G., Huang, L.J., Chen, K., Tang, Y., Pi, X., Yang, R., Peng, X., Cui, C., Li, N., 2024. Unveiling the toxic effects, physiological responses and molecular mechanisms of tobacco (*Nicotiana tabacum*) in exposure to organic ultraviolet filters. J. Hazard Mater. 465, 133060. https://doi.org/10.1016/j.jhazmat.2023.133060.

Jovanovic, B., Guzman, H.M., 2014. Effects of titanium dioxide (TiO_2) nanoparticles on caribbean reef-building coral (*Montastraea faveolata*). Environ. Toxicol. Chem. 33 (6), 1346–1353. https://doi.org/10.1002/etc.2560.

Kanehisa, M., Araki, M., Goto, S., Hattori, M., Hirakawa, M., Itoh, M., Katayama, T., Kawashima, S., Okuda, S., Tokimatsu, T., Yamanishi, Y., 2008. KEGG for linking genomes to life and the environment. Nucleic Acids Res. 36 (Database issue), D480–D484. https://doi.org/10.1093/nar/gkm882.

Kaniewska, P., Chan, C.-K.K., Kline, D., Ling, E.Y.S., Rosic, N., Edwards, D., Hoegh-Guldberg, O., Dove, S., 2015. Transcriptomic changes in coral holobionts provide insights into physiological challenges of future climate and ocean change. PLoS One 10 (10), e0139223. https://doi.org/10.1371/journal.pone.0139223.

Labille, J., Catalano, R., Slomberg, D., Motellier, S., Pinsino, A., Hennebert, P., Santaella, C., Bartolomei, V., 2020. Assessing sunscreen lifecycle to minimize environmental risk posed by nanoparticulate UV-filters–a review for safer-by-design products. Front. Environ. Sci. 8. https://doi.org/10.3389/fenvs.2020.00101.

Li, K., Xu, D., Liao, H., Xue, Y., Sun, M., Su, H., Xiu, X., Zhao, T., 2022. A review on the generation, discharge, distribution, environmental behavior, and toxicity (especially to microbial aggregates) of nano-TiO_2 in sewage and surface-water and related research prospects. Sci. Total Environ. 824, 153866. https://doi.org/10.1016/j.scitotenv.2022.153866.

Li, Z., Hu, M., Song, H., Lin, D., Wang, Y., 2021. Toxic effects of nano-TiO_2 in bivalves-A synthesis of meta-analysis and bibliometric analysis. J. Environ. Sci. 104, 188–203. https://doi.org/10.1016/j.jes.2020.11.013.

Lin, Y., Miao, L.H., Pan, W.J., Huang, X., Dengu, J.M., Zhang, W.X., Ge, X.P., Liu, B., Ren, M.C., Zhou, Q.L., Xie, J., Pan, L.K., Xi, B.W., 2018. Effect of nitrite exposure on the antioxidant enzymes and glutathione system in the liver of bighead carp, *Aristichthys nobilis*. Fish Shellfish Immunol. 76, 126–132. https://doi.org/10.1016/j.fsi.2018.02.015.

Liu, X., Wu, L., Si, Y., Zhai, Y., Niu, M., Han, M., Su, T., 2024. Regulating effect of exogenous α-ketoglutarate on ammonium assimilation in poplar. Molecules 29 (7), 1425. https://doi.org/10.3390/molecules29071425.

López-Alonso, J.P., Lázaro, M., Gil-Cartón, D., Choi, P.H., Dodu, A., Tong, L., Valle, M., 2022. CryoEM structural exploration of catalytically active enzyme pyruvate carboxylase. Nat. Commun. 13 (1), 6185. https://doi.org/10.1038/s41467-022-33987-2.

Love, M.I., Huber, W., Anders, S., 2014. Moderated estimation of fold change and dispersion for RNA-seq data with DESeq2. Genome Biol. 15 (12), 550. https://doi.org/10.1186/s13059-014-0550-8.

Lu, Y., Luo, F., Yang, M., Li, X., Lian, X., 2011. Suppression of glutamate synthase genes significantly affects carbon and nitrogen metabolism in rice (*Oryza sativa L.*). Sci. China Life Sci. 54, 651–663. https://doi.org/10.1007/s11427-011-4191-9.

Luo, Z., Li, Z., Xie, Z., Sokolova, I.M., Song, L., Peijnenburg, W., Hu, M., Wang, Y., 2020. Rethinking nano-TiO_2 safety: overview of toxic effects in humans and aquatic animals. Small 16 (36), e2002019. https://doi.org/10.1002/smll.202002019.

Ma, C., Ban, T., Yu, H., Li, Q., Li, X., Jiang, W., Xie, J., 2019. Urea addition promotes the metabolism and utilization of nitrogen in cucumber. Agronomy 9 (5), 262. https://doi.org/10.3390/agronomy9050262.

Mansfield, K.M., Gilmore, T.D., 2019. Innate immunity and cnidarian-Symbiodiniaceae mutualism. Dev. Comp. Immunol. 90, 199–209. https://doi.org/10.1016/j.dci.2018.09.020.

Marcellini, F., Varrella, S., Ghilardi, M., Barucca, G., Giorgetti, A., Danovaro, R., Corinaldesi, C., 2024. Inorganic UV filter-based sunscreens labelled as eco-friendly threaten sea urchin populations. Environ. Pollut. 351, 124093. https://doi.org/10.1016/j.envpol.2024.124093.

Matyas, C., Haskó, G., Liaudet, L., Trojnar, E., Pacher, P., 2021. Interplay of cardiovascular mediators, oxidative stress and inflammation in liver disease and its complications. Nat. Rev. Cardiol. 18 (2), 117–135. https://doi.org/10.1038/s41569-020-0433-5.

May, L.A., Burnett, A.R., Miller, C.V., Pisarski, E., Webster, L.F., Moffitt, Z.J., Pennington, P., Wirth, E., Baker, G., Ricker, R., Woodley, C.M., 2020. Effect of Louisiana sweet crude oil on a Pacific coral, *Pocillopora damicornis*. Aquat. Toxicol. 222, 105454. https://doi.org/10.1016/j.aquatox.2020.105454.

Mironava, T., Hadjiargyrou, M., Simon, M., Jurukovski, V., Rafailovich, M.H., 2010. Gold nanoparticles cellular toxicity and recovery: effect of size, concentration and exposure time. Nanotoxicology 4 (1), 120–137. https://doi.org/10.3109/17435390903471463.

Moeller, M., Pawlowski, S., Petersen-Thiery, M., Miller, I.B., Nietzer, S., Heisel-Sure, Y., Kellermann, M.Y., Schupp, P.J., 2021. Challenges in current coral reef

protection–possible impacts of UV filters used in sunscreens, a critical review. Front. Mar. Sci. https://doi.org/10.3389/fmars.2021.665548.
Molina, V.H., Castillo-Medina, R.E., Thomé, P.E., 2017. Experimentally induced bleaching in the sea anemone *Exaiptasia* supports glucose as a main metabolite associated with its symbiosis. J. Mar. Sci. 2017 (1), 3130723. https://doi.org/10.1155/2017/3130723.
Nel, A., Xia, T., Mädler, L., Li, N., 2006. Toxic potential of materials at the nanolevel. Science 311 (5761), 622–627. https://doi.org/10.1126/science.1114397.
Palmer, C., Traylor-Knowles, N., 2012. Towards an integrated network of coral immune mechanisms. Proc. Biol. Sci. 279 (1745), 4106–4114. https://doi.org/10.1098/rspb.2012.
Pei, J., Yu, W., Zhang, J., Kuo, T., Chung, H., Hu, J., Hsu, C., Yu, K., 2022a. Mass spectrometry–based metabolomic signatures of coral bleaching under thermal stress. Anal. Bioanal. Chem. 414 (26), 7635–7646. https://doi.org/10.1007/s00216-022-04294-y.
Pei, Y., Chen, S., Zhang, Y., Olga, V., Li, Y., Diao, X., Zhou, H., 2022b. Coral and it's symbionts responses to the typical global marine pollutant BaP by 4D-Proteomics approach. Environ. Pollut. 307, 119440. https://doi.org/10.1016/j.envpol.2022.119440.
Polato, N.R., Voolstra, C.R., Schnetzer, J., DeSalvo, M.K., Randall, C.J., Szmant, A.M., Medina, M., Baums, I.B., 2010. Location-specific responses to thermal stress in larvae of the reef-building coral *Montastraea faveolata*. PLoS One 5 (6), e11221. https://doi.org/10.1371/journal.pone.0011221.
Puntin, G., Craggs, J., Hayden, R., Engelhardt, K.E., McIlroy, S., Sweet, M., Baker, D.M., Ziegler, M., 2022. The reef-building coral *Galaxea fascicularis*: a new model system for coral symbiosis research. Coral Reefs 42 (1), 239–252. https://doi.org/10.1007/s00338-022-02334-8.
Qin, Z., Yu, K., Wang, Y., Xu, L., Huang, X., Chen, B., Li, Y., Wang, W., Pan, Z., 2019. Spatial and intergeneric variation in physiological indicators of corals in the South China Sea: insights into their current state and their adaptability to environmental stress. J. Geophys. Res.: Oceans 124, 3317–3332. https://doi.org/10.1029/2018JC014648.
Rauta, P.R., Samanta, M., Dash, H.R., Nayak, B., Das, S., 2014. Toll-like receptors (TLRs) in aquatic animals: signaling pathways, expressions and immune responses. Immunol. Lett. 158 (1), 14–24. https://doi.org/10.1016/j.imlet.2013.11.013.
Roberto, D., Lucia, B., Cinzia, C., Donato, G., Elisabetta, D., Paola, A., Lucedio, G., Antonio, P., 2008. Sunscreens cause coral bleaching by promoting viral infections. Environ. Health Perspect. 116, 441–447. https://doi.org/10.1289/ehp.10966.
Sanchez-Quiles, D., Tovar-Sanchez, A., 2014. Sunscreens as a source of hydrogen peroxide production in coastal waters. Environ. Sci. Technol. 48 (16), 9037–9042. https://doi.org/10.1021/es5020696.
Saskia, H., Patten, N.L., Waite, A.M., Fabiano, T., 2013. Temporal variations in metabolic and autotrophic indices for *Acropora digitifera* and *Acropora spicifera*-implications for monitoring projects. PLoS One 8 (5), e63693. https://doi.org/10.1371/journal.pone.0063693.
Schneider, S.L., Lim, H.W., 2019. A review of inorganic UV filters zinc oxide and titanium dioxide. Photodermatol. Photoimmunol. Photomed. 35 (6), 442–446. https://doi.org/10.1111/phpp.12439.
Sendra, M., Sanchez-Quiles, D., Blasco, J., Moreno-Garrido, I., Lubian, L.M., Perez-Garcia, S., Tovar-Sanchez, A., 2017. Effects of TiO_2 nanoparticles and sunscreens on coastal marine microalgae: ultraviolet radiation is key variable for toxicity assessment. Environ. Int. 98, 62–68. https://doi.org/10.1016/j.envint.2016.09.024.
Sobkowicz, A.D., Gallagher, M.E., Reid, C.J., Crean, D., Carrington, S.D., Irwin, J.A., 2014. Modulation of expression in BEAS-2B airway epithelial cells of α-l-fucosidase A1 and A2 by Th1 and Th2 cytokines, and overexpression of α-l-fucosidase 2. Mol. Cell. Biochem. 390 (1), 101–113. https://doi.org/10.1007/s11010-014-1961-2.
Stien, D., Clergeaud, F., Rodrigues, A.M.S., Lebaron, K., Pillot, R., Romans, P., Fagervold, S., Lebaron, P., 2019. Metabolomics reveal that octocrylene accumulates in *Pocillopora damicornis* tissues as fatty acid conjugates and triggers coral cell mitochondrial dysfunction. Anal. Chem. 91 (1), 990–995. https://doi.org/10.1021/acs.analchem.8b04187.
Sun, T.Y., Bornhöft, N.A., Hungerbühler, K., Nowack, B., 2016. Dynamic probabilistic modeling of environmental emissions of engineered nanomaterials. Environ. Sci. Technol. 50 (9), 4701–4711. https://doi.org/10.1021/acs.est.5b05828.
Sun, Y., Jiang, L., Gong, S., Diaz-Pulido, G., Yuan, X., Tong, H., Huang, L., Zhou, G., Zhang, Y., Huang, H., 2022. Changes in physiological performance and protein expression in the larvae of the coral *Pocillopora damicornis* and their symbionts in response to elevated temperature and acidification. Sci. Total Environ. 807, 151251. https://doi.org/10.1016/j.scitotenv.2021.151251.
Takasu, H., Nakata, K., Ito, M., Yasui, M., Yamaguchi, M., 2023. Effects of TiO_2 and ZnO nanoparticles on the growth of phytoplankton assemblages in seawater. Mar. Environ. Res. 183, 105826. https://doi.org/10.1016/j.marenvres.2022.105826.
Tang, J., Ni, X., Zhou, Z., Wang, L., Lin, S., 2018. Acute microplastic exposure raises stress response and suppresses detoxification and immune capacities in the scleractinian coral *Pocillopora damicornis*. Environ. Pollut. 243, 66–74. https://doi.org/10.1016/j.envpol.2018.08.045.
Vuckovic, D., Tinoco, A.I., Ling, L., Renicke, C., Pringle, J.R., Mitch, W.A., 2022. Conversion of oxybenzone sunscreen to phototoxic glucoside conjugates by sea anemones and corals. science 376, 644–648. https://doi.org/10.1126/science.abn2600.
Wan, J., Wang, R., Wang, R., Ju, Q., Wang, Y., Xu, J., 2019. Comparative physiological and transcriptomic analyses reveal the toxic effects of ZnO nanoparticles on plant growth. Environ. Sci. Technol. 53 (8), 4235–4244. https://doi.org/10.1021/acs.est.8b06641.
Wang, W., Tang, K., Wang, P., Zeng, Z., Xu, T., Zhan, W., Liu, T., Wang, Y., Wang, X., 2022. The coral pathogen *Vibrio coralliilyticus* kills non-pathogenic holobiont competitors by triggering prophage induction. Nat. Ecol. Evol. https://doi.org/10.1038/s41559-022-01795-y.
Wang, X., Zhang, D., Jiang, N., Wang, X., Zhang, N., Zhang, K., Sang, X., Feng, Y., Chen, R., Yang, N., Chen, Q., 2021. Induction of apoptosis in *Trypanosoma brucei* following endocytosis of ultra-small noble metal nanoclusters. Nano Today 38, 101122. https://doi.org/10.1016/j.nantod.2021.101122.
Wei, W., Wu, H., Xu, H., Xu, T., Zhang, X., Chang, K., Zhang, Y., 2009. Cloning and molecular characterization of two complement Bf/C2 genes in large yellow croaker (*Pseudosciaena crocea*). Fish Shellfish Immunol. 27 (2), 285–295. https://doi.org/10.1016/j.fsi.2009.05.011.
Wright, R.M., Kenkel, C.D., Dunn, C.E., Shilling, E.N., Bay, L.K., Matz, M.V., 2017. Intraspecific differences in molecular stress responses and coral pathobiome contribute to mortality under bacterial challenge in *Acropora millepora*. Sci. Rep. 7 (1), 2609. https://doi.org/10.1038/s41598-017-02685-1.
Wu, F., Kong, H., Xie, L., Sokolova, I.M., 2024. Exposure to nanopollutants (nZnO) enhances the negative effects of hypoxia and delays recovery of the mussels' immune system. Environ. Pollut. 351, 124112. https://doi.org/10.1016/j.envpol.2024.124112.
Wu, F., Sokolov, E.P., Khomich, A., Fettkenhauer, C., Schnell, G., Seitz, H., Sokolova, I. M., 2022. Interactive effects of ZnO nanoparticles and temperature on molecular and cellular stress responses of the blue mussel *Mytilus edulis*. Sci. Total Environ. 818, 151785. https://doi.org/10.1016/j.scitotenv.2021.151785.
Xiong, D., Fang, T., Yu, L., Sima, X., Zhu, W., 2011. Effects of nano-scale TiO_2, ZnO and their bulk counterparts on zebrafish: acute toxicity, oxidative stress and oxidative damage. Sci. Total Environ. 409 (8), 1444–1452. https://doi.org/10.1016/j.scitotenv.2011.01.015.
Yin, H., Casey, P.S., McCall, M.J., Fenech, M., 2010. Effects of surface chemistry on cytotoxicity, genotoxicity, and the generation of reactive oxygen species induced by ZnO nanoparticles. Langmuir 26 (19), 15399–15408. https://doi.org/10.1021/la101033n.
Yu, X., Jiang, L., Gan, J., Zhang, Y., Luo, Y., Liu, C., Huang, H., 2021. Effects of feeding on production, body composition and fatty acid profile of scleractinian coral *Galaxea fascicularis*. Aquac. Rep. 21, 100871. https://doi.org/10.1016/j.aqrep.2021.100871.
Yu, X., Yu, K., Liao, Z., Liang, J., Deng, C., Huang, W., Huang, Y., 2020. Potential molecular traits underlying environmental tolerance of *Pavona decussata* and *Acropora pruinosa* in Weizhou Island, northern South China Sea. Mar. Pollut. Bull. 156, 111199. https://doi.org/10.1016/j.marpolbul.2020.111199.
Yuan, S., Huang, J., Jiang, X., Huang, Y., Zhu, X., Cai, Z., 2022. Environmental fate and toxicity of sunscreen-derived inorganic ultraviolet filters in aquatic environments: a Review. Nanomaterials 12 (4). https://doi.org/10.3390/nano12040699.
Yuan, S., Huang, J., Qian, W., Zhu, X., Wang, S., Jiang, X., 2023. Are physical sunscreens safe for marine life? A study on a coral–zooxanthellae symbiotic system. Environ. Sci. Technol. 57 (42), 15846–15857. https://doi.org/10.1021/acs.est.3c04603.
Zhang, R., Yu, K., Li, A., Wang, Y., Huang, X., 2019. Antibiotics in corals of the South China Sea: occurrence, distribution, bioaccumulation, and considerable role of coral mucus. Environ. Pollut. 250, 503–510. https://doi.org/10.1016/j.envpol.2019.04.036.
Zhang, Y., Hu, J., Li, Y., Zhang, M., Jacques, K.J., Gu, W., Sun, Y., Sun, J., Yang, Y., Xu, S., Wang, Y., Yan, X., 2021. Immune response of silver pomfret (*Pampus argenteus*) to *Amyloodinium ocellatum* infection. J. Fish. Dis. 44 (12), 2111–2123. https://doi.org/10.1111/jfd.13524.
Zhang, Y., Ke, H., Qin, Y., Ju, H., Chen, Y., Lin, F., Zhang, J., Diao, X., 2023. Environmental concentrations of benzophenone-3 disturbed lipid metabolism in the liver of clown anemonefish (*Amphiprion ocellaris*). Environ. Pollut. 317, 120792. https://doi.org/10.1016/j.envpol.2022.120792.